Effect of the Structure on the Morphology and Spherulitic Growth Kinetics of Polyolefin In-Reactor Alloys

Jun-Ting Xu, Zhi-Sheng Fu, Xian-Ping Wang, Jun-Sheng Geng, Zhi-Qiang Fan

Department of Polymer Science and Engineering, Zhejiang University, Hangzhou 310027, China

Received 1 October 2004; accepted 6 February 2005
DOI 10.1002/app.22074
Published online in Wiley InterScience (www.interscience.wiley.com).

ABSTRACT: Four polyolefin in-reactor alloys with different compositions and structures were prepared by sequential polymerization. All the alloys were fractionated into five fractions: a random copolymer of ethylene and propylene (25°C fraction), an ethylene–propylene segmented copolymer (90°C fraction), an ethylene homopolymer (110°C fraction), an ethylene–propylene block copolymer (120°C fraction), and a propylene homopolymer plus a minor ethylene homopolymer of high molecular weight (>120°C fraction). The effect of the structure on the morphology and spherulitic growth kinetics of the polypropylene (PP) component in the alloys was investigated. The polyolefin alloys containing a suitable block copolymer fraction and a larger amount of PP had a more homogeneous morphology, and the crystalline particles were smaller. Quenching the polyolefin alloys led to smaller crystallites and a more homogeneous morphology as well. Isothermal crystallization was carried out above the melting temperature of polyethylene, and the growth of PP spherulites was monitored with polarized optical microscopy with a hot stage. The alloys with higher propylene contents exhibited a faster spherulitic growth rate. The fold surface free energy was derived, and it was found that a large amount of block copolymer fractions and random copolymer fractions could reduce the fold surface free energy. The structure of the alloys also affected the crystallization regime of PP. © 2005 Wiley Periodicals, Inc. J Appl Polym Sci 98: 632–638, 2005

Key words: alloys; crystallization; morphology; poly(propylene) (PP); spherulites

INTRODUCTION

It is well known that propylene homopolymer has poor impact properties, especially at low temperatures. To improve the impact properties of polypropylene (PP), PP alloys have been developed by the sequential polymerization of propylene and ethylene and/or the copolymerization of ethylene and propylene.[1,2] PP alloys can exhibit excellent mechanical properties in both impact and tensile tests because of the unique morphology of the alloys[3] and the existence of some special components, such as an ethylene–propylene block copolymer.[4–6] Because of the nonliving characteristic of coordination polymerization, PP alloys prepared by sequential copolymerization are usually a mixture of a propylene homopolymer, an ethylene homopolymer, an ethylene–propylene random copolymer, an ethylene–propylene segmented copolymer, and an ethylene–propylene block copolymer.[7–12] A study of the relationship between the structure and properties is very important because it can help us understand the origin of the excellent mechanical properties of high-impact PP and may provide some basic ideas for the design of new materials. However, so far most studies have concentrated on the properties of the separated fractions with different structures,[13–17] or the properties of polyolefin alloys have only been correlated with the overall composition or the content of the rubber component.[18,19] There have been few reports on the effect of block copolymer fractions on the morphology and properties of PP alloys,[20,21] partially because of the complicated microstructure and morphology of PP alloys. In our previous work, we prepared polyolefin alloys by the sequential polymerization method, and polyolefin in-reactor alloys with different structures and compositions were obtained.[22] For example, polyethylene (PE)/PP in-reactor alloys were prepared by a three-stage polymerization process: prepolymerization of propylene in slurry, gas-phase homopolymerization of ethylene, and gas-phase homopolymerization of propylene.[22] When this polymerization process was followed by a fourth stage of ethylene–propylene copolymerization, PE/PP/ethylene-propylene random copolymer (EPR) in-reactor alloys with a high quantity of an ethylene–propylene random copolymer were prepared.[23] By changing the polymerization conditions, we can readily control the composition of the

Correspondence to: J.-T. Xu (xujt@zju.edu.cn).
Contract grant sponsor: Special Funds for Major State Basic Research Projects; contract grant number: G1999064803.
Contract grant sponsor: Scientific Research Foundation for the Returned Overseas Chinese Scholars of the State Education Ministry.

in-reactor alloys. In this study, PE/PP and PE/PP/EPR in-reactor alloys with different structures were prepared, and the effect of the structure on the morphology of the alloys was studied. Moreover, to facilitate the study, isothermal crystallization was carried out above the melting temperature of PE, and the spherulitic growth kinetics of PP were correlated with the structure of the alloys.

EXPERIMENTAL

Preparation of the PP alloys

The PE/PP in-reactor alloys (samples A and B) were synthesized in a three-stage polymerization process. In the first stage, or the prepolymerization stage, the slurry polymerization of propylene was conducted in a well-stirred glass reactor for 30 min. A high-yield spherical Ziegler–Natta catalyst, $TiCl_4/MgCl_2 \cdot ID$ (ID is internal donor diisobutyl phthalate), kindly donated by the Beijing Research Institute of Chemical Industry (Beijing, China), was used in the polymerization. The catalyst had a Ti content of 3.0 wt %. $Al(C_2H_5)_3$ (Fluka, Japan) was used as the cocatalyst (with Al/Ti = 60), and $(C_6H_5)_2Si(OCH_3)_2$ was used as the external donor (Al/Si = 25). Petroleum ether (30 mL; bp = 60–90°C) was used as the solvent. The propylene pressure in the prepolymerization stage was 1 atm, and the temperature was 50°C. A catalyst efficiency of 15–20 g of PP/g of catalyst was obtained in this stage. After the prepolymerization, the slurry containing the prepolymerized catalyst was transferred to a Büchiglasuster 0.5-L jacketed autoclave (Uster, Switzerland). Propylene in the slurry was removed by the evacuation of the autoclave to 5 mmHg for 3 s, and ethylene was filled into the autoclave to 0.6 MPa. Ethylene homopolymerization was carried out for 1 h. For sample A, the polymerization temperature was 70°C, and for sample B, the polymerization temperature was 60°C. Because the polymerization rates were different at various polymerization temperatures, the polymerization temperature could be used to regulate the PE content in the in-reactor alloys. After about 20 min of ethylene polymerization, all the petroleum ether in the reactor was thoroughly absorbed into the polymer granules, so the polymerization could be regarded as a gas-phase process. At the end of this stage, ethylene was removed by evacuation to 5 mmHg for 3 min, and propylene was let into the autoclave and then continuously supplied to the reactor at 0.7 MPa for 2 h. After the gas-phase propylene polymerization stage, the reaction was terminated, and the product was washed with ethanol and dried *in vacuo*. The preparation of the PE/PP/EPR in-reactor alloys (samples C and D) was similar to that of sample B, except that a fourth stage of copolymerization of ethylene and propylene was added. After the gas-phase propylene polymerization, propylene was removed by evacuation to 5 mmHg for 3 min, and an ethylene–propylene mixture of constant composition (ethylene/propylene = 1) was continuously supplied to the autoclave at 60°C. The pressure of the ethylene–propylene mixture for PE/PP/EPR was 0.7 MPa for sample D and 0.4 MPa for sample C. After ethylene–propylene copolymerization for 1 h, the reaction was terminated, and the product was washed with ethanol and dried *in vacuo*.

Characterization of the PP alloys

A modified Kumagawa extractor was used to carry out temperature-gradient extraction fractionation of the polymers.[24] *n*-Octane was used as the solvent to successively extract the samples at different controlled temperatures (room temperature and 90, 110, and 120°C). Five fractions were collected at 25, 90, 110, 120, and >120°C from each alloy, the >120°C fraction being the residual after the extraction. The fractions were named the 25°C fraction, 90°C fraction, 110°C fraction, 120°C fraction, and >120°C fraction. Purified fractions were obtained after the extract solutions were concentrated, the polymers were precipitated, and the fractions were washed and dried *in vacuo*. ^{13}C-NMR spectra of the fractions were measured on a Bruker AMX500 NMR spectrometer (Rheinstetten, Germany) at 100 MHz. *o*-Dichlorobenzene-d_4 was used as the solvent to prepare polymer solutions of 20 wt %. The spectra were recorded at 120°C, with hexamethyldisiloxane as an internal reference. Broadband decoupling and a pulse delay of 5 s were employed. Typically, 1000 transients were collected. The ethylene content of the samples was determined on the basis of the peak area data. The thermal behavior of the PP alloys was characterized with a PerkinElmer Pyris-1 differential scanning calorimeter (Boston, MA). The samples were first heated to 200°C and held for 5 min to remove the thermal history. Subsequently, the samples were cooled to room temperature at a rate of 10°C/min and then heated to 180°C at a rate of 10°C/min. The differential scanning calorimetry (DSC) traces were recorded upon cooling and melting.

Polarized optical microscopy (POM)

An Olympus BX-5 polarized optical microscope (Tokyo, Japan) equipped with a hot stage and a digital camera was used to study the morphology of the alloys under nonisothermal and isothermal crystallization conditions. For nonisothermal crystallization, the in-reactor alloys, covered by glass slices, were first melted at 200°C on the hot stage; then, the samples

TABLE I
Fraction Distribution and Composition of the Fractions in the PE/PP and PE/PP/EPR Alloys

	Percentage of fractions (wt %)				Ethylene content in fractions (wt %)			
Fraction (°C)	A	B	C	D	A	B	C	D
25	0.2	0.3	15.7	7.0	81.7	24.6	20.2	36.4
90	4.1	3.4	14.9	14.2	49.7	48.4	34.3	52.1
110	47.1	37.7	33.4	22.9	96.2	93.7	96.0	95.6
120	47.5	25.4	24.7	47.7	69.2	24.9	69.0	92.4
>120	1.1	33.2	11.3	8.2	88.9	0.6	6.1	4.3

were quenched with ice water or were left on the hot stage, with the power switched off, and slowly cooled in air. Under isothermal crystallization, the samples were first melted at 200°C on the hot stage and were then transferred to another hot stage at the preset crystallization temperature (T_c) and allowed to crystallize isothermally. The hot stage was calibrated with standard, sharp-melting substances. The temperature fluctuation was within ±1°C. During crystallization, the growth of the spherulites was monitored as a function of time. The linear growth rate, $G = dR(t)/dt$, was calculated according to the following equation:

$$R(t) = R_0 + G(T_c)(t - t_0) \quad (1)$$

where $R(t)$ is the spherulite radius; t is the time; and R_0 is the so-called offset radius, which is the radius of the spherulite already growing during the period of cooling at the time when the sample reaches T_c (t_0). In all cases, the average growth rate was determined from the slope of the plots of $R(t)$ versus t. The values of t_0 could vary with the experimental runs, but this did not matter because we were only interested in the slope G.

RESULTS AND DISCUSSION

Composition and thermal behavior of the polyolefin alloys

Table I summarizes the fractionation results and the compositions of the fractions determined by ^{13}C-NMR. The composition and structure of the fractions have been analyzed in our previous wok.[22] The 25°C fraction is a random copolymer of ethylene and propylene, and the 90°C fraction is an ethylene–propylene segmented copolymer, in which both the ethylene and propylene segments are crystallizable but show lower melting temperatures. The 110°C fraction is mainly an ethylene homopolymer, and the 120°C fraction is an ethylene–propylene block copolymer. The >120°C fraction is a propylene homopolymer plus an ethylene homopolymer of high molecular weight. Comparing the compositions of the two PE/PP in-reactor alloys, we can see that B is a mixture of an ethylene homopolymer, an ethylene–propylene block copolymer, and a propylene homopolymer, whereas sample A mainly contains an ethylene homopolymer and an ethylene–propylene block copolymer. There is little propylene homopolymer in sample A, and most of the propylene units in A exist in the form of a block copolymer. There is a larger amount of the 120°C fraction (ethylene–propylene block copolymer) in sample A than in B, and this fraction contains more ethylene than the 120°C fraction obtained by B. The PE/PP/EPR alloys are richer in the 25°C fraction (ethylene–propylene random copolymer) and 90°C fraction (ethylene–propylene segmented copolymer) than the PE/PP alloys. Such a composition is in accordance with the preparation procedure of the PE/PP/EPR alloys because the copolymerization of ethylene and propylene was conducted in the last stage. The most obvious differences in the compositions of these two PE/PP/EPR alloys are the larger amount of the ethylene–propylene block copolymer fraction and a very small content of propylene units in the block copolymer fraction of sample D with respect to sample C. The latter contains more of the ethylene homopolymer fraction and random copolymer fraction than sample D.

The crystallization and subsequent melting DSC traces of the overall polyolefin alloys are shown in Figures 1 and 2, respectively. The crystallization peaks of the ethylene and propylene segments are unresolved. However, their melting peaks are well separated. The intensity of the PP peak with respect to that of PE increases with the content of PP in the alloys. In sample A, the melting peak of PP is very weak, in accordance with its small amount of PP. In the other three alloys, the melting peak of PP is quite obvious. The smaller amount of PP also leads to a slightly lower melting temperature of PP.

Morphology after nonisothermal crystallization

Figure 3 shows POM micrographs of the polyolefin in-reactor alloys quenched from the melt and slowly cooled in the air. A nonuniform morphology can be observed for all the polyolefin alloys because of the temperature decrease during crystallization. The quenched samples crystallize less perfectly and show smaller crystalline particles than the slowly cooled samples. For example, no spherulites are observable in

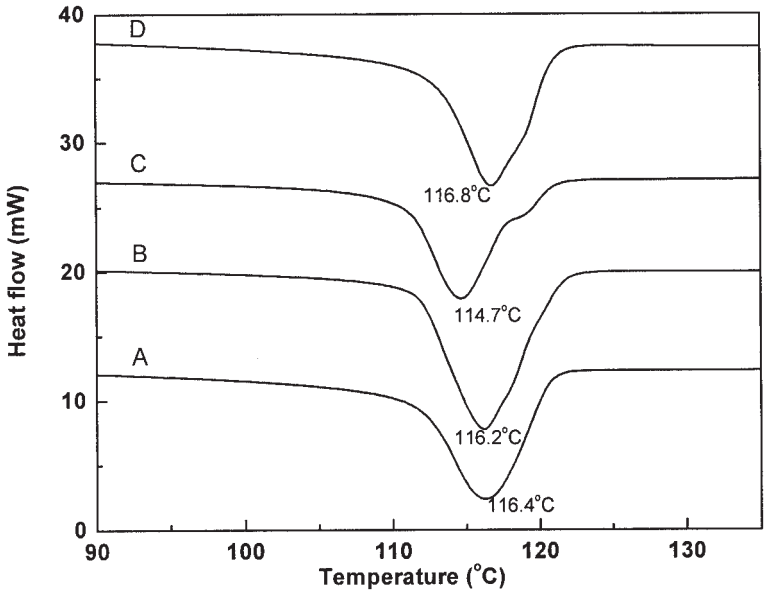

Figure 1 Cooling DSC traces of the polyolefin in-reactor alloys.

quenched sample A, but spherulites can be seen in slowly cooled sample A. Comparing the morphology of samples A and B, we can see that the crystalline particles of sample A are larger than those of sample B. There are no spherulites even in slowly cooled sample B, and the crystalline particles are small even under slowly cooled crystallization conditions. Moreover, the size distribution of the crystalline particles in sample B is much more homogeneous than that in A. On the basis of DSC results, we know that sample B contains more crystalline PP domains, which can act as nucleation reagents; thus, the size of PE spherulites in sample B is smaller and more uniform.

For the two PE/PP/EPR in-reactor alloys, sample C exhibits a nonspherulitic morphology when quenched from the melt, but spherulites are formed under slowly cooling conditions. Spherulites can be observed in both quenched and slowly cooled sample D, but spherulites are more evident under slowly cooling conditions. In Figure 3(h), the larger spherulites are banded, and so they must consist of PE. Apparently, the nonuniform morphology is more accentuated in

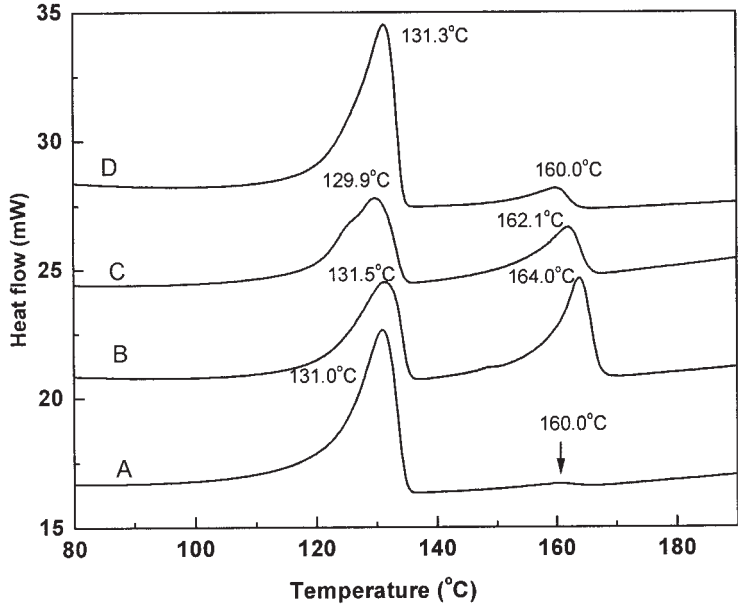

Figure 2 Melting DSC traces of the polyolefin in-reactor alloys.

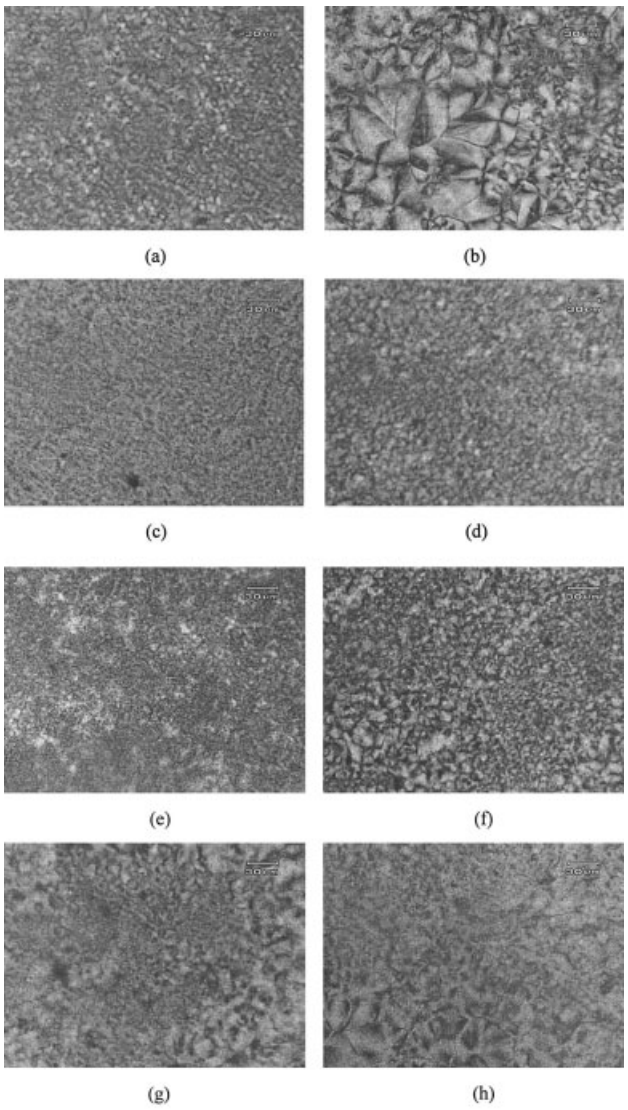

Figure 3 POM micrographs of PE/PP and PE/PP/EPR in-reactor alloys after nonisothermal crystallization (bar = 30 μm): (a) sample A (quenched), (b) sample A (slowly cooled), (c) sample B (quenched), (d) sample B (slowly cooled), (e) sample C (quenched), (f) sample C (slowly cooled), (g) sample D (quenched), and (h) sample D (slowly cooled).

sample D because of its higher content of crystallizable ethylene units in the block copolymer fraction (120°C fraction) with respect to sample C.

Linear growth rate of the PP spherulites

The aforementioned results shows that there are some differences in the morphology for the polyolefin in-reactor alloys with different compositions. However, because in the PE/PP and PE/PP/EPR alloys both PE and PP in various fractions (block copolymers and homopolymers) can crystallize, this leads to a complicated ultimate morphology of the in-reactor alloys and makes it difficult to correlate the structure and morphology. To simplify the situation and to facilitate a correlation between the structure and properties, isothermal crystallization was conducted in temperature ranges in which only PP was crystallizable and PE could not crystallize, and the spherulitic growth kinetics of PP were studied. However, the DSC characterization reveals that the T_c ranges of PE and PP in the alloys severely overlap. In this work, most T_c's of PP are above the melting temperature of PE, that is, higher than 132°C. Spherulites are formed under isothermal crystallization conditions for all four PP in-reactor alloys. Figure 4 exemplifies the spherulitic morphology of sample C at different crystallization times, and Figure 5 illustrates changes in the spherulite diameter with time for sample C at various T_c's. Table II summarizes the linear growth of spherulites of different PP in-reactor alloys. In the T_c range studied, sample B has larger G values than sample A, and the values of G for sample C are larger than those for sample D. The larger G values of B and C result from their higher weight percentages of propylene homopolymer.

From the G value of the spherulite, the effect of the composition of the polyolefin in-reactor alloys on the fold surface free energy (σ_e) can be evaluated. The relationship between σ_e and G of the spherulite at T_c is[25,26]

$$G = G_0 \exp[-U^*/R(T_c - T_0)] \exp[-K_g/T_c(\Delta T)f] \quad (2)$$

where G_0 is a constant and is independent of the temperature; U^* is the activation energy related to the short-distance diffusion of the crystalline unit across

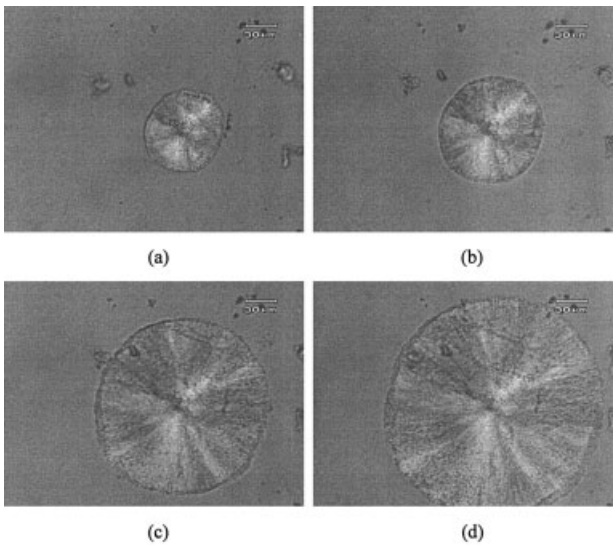

Figure 4 Spherulitic morphology of sample C during isothermal crystallization at 146°C (bar = 30 μm): (a) 20 s, (b) 120 s, (c) 300 s, and (d) 630 s.

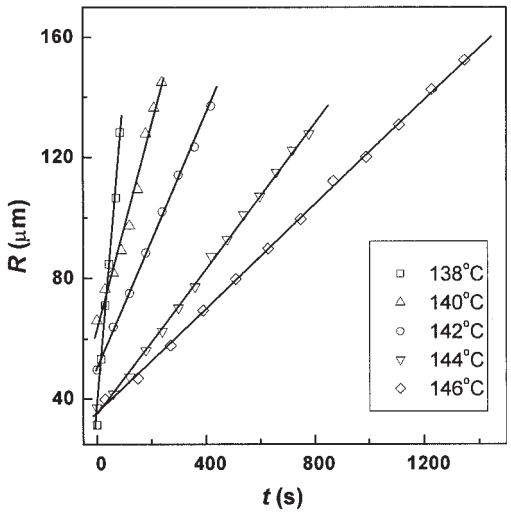

Figure 5 Plots of the spherulitic radius (R) versus the crystallization time (t) for sample C at various temperatures.

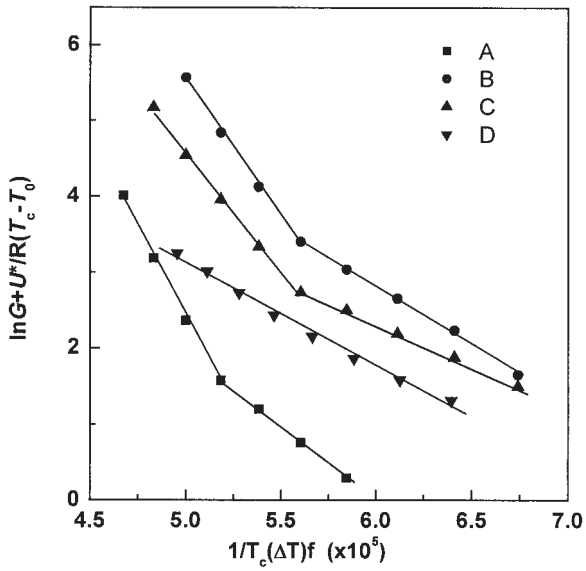

Figure 6 Plots of $\ln G + U^*/R(T_c - T_0)$ versus $1/T_c(\Delta T)f$ for PE/PP and PE/PP/EPR in-reactor alloys.

the phase boundary; T_0 is the temperature below which there is no chain motion (usually $T_0 = T_g - 30$ K); ΔT is the supercooling ($\Delta T = T_m^0 - T_c$), that is, the difference between the equilibrium melting temperature (T_m^0) and T_c; and f is the correction factor and is equal to $2T_c/(T_m^0 + T_c)$. Equation (2) can be reformed into

$$\ln G + U^*/R(T_c - T_0) = \ln G_0 - K_g/T_c(\Delta T)f \quad (3)$$

As a result, the nucleation constant (K_g) can be obtained from the slope of the plot of $\ln G + U^*/R(T_c - T_0)$ versus $1/T_c(\Delta T)f$.

K_g can also be expressed as follows:[27]

$$K_g = jb_0\,\sigma\sigma_e T_m^0/k(\Delta h_f) \quad (4)$$

where j is 4 for crystallization regimes I and III and j is 2 for crystallization regime II, b_0 is the layer thickness, σ is the lateral surface free energy, Δh_f is the fusion enthalpy, and k is Boltzmann's constant. The values of U^*, T_m^0, T_0, Δh_f, b_0, and σ are 6.28 kJ/mol, 458.2 K, 231.2 K, 1.96×10^8 J/m^3, 6.26 Å, and 11.5 erg/cm^2, respectively.[25,27–29]

The chain folding work (q) can be determined with the following equation:[30]

$$q = 2\sigma_e\, a_0 b_0 \quad (5)$$

where a_0 is the width of the PP chain stem, which is 5.49 Å.[27]

Figure 6 shows the plots of $\ln G + U^*/R(T_c - T_0)$ versus $1/T_c(\Delta T)f$ for these four PP in-reactor alloys. The transition temperature from crystallization regime II to crystallization regime III ($T_{II\to III}$), σ_e, and q are given in Table III. First, we notice that these four PP in-reactor alloys have different values of $T_{II\to III}$. The alloy with a higher weight percentage of PP has higher $T_{II\to III}$. For example, the value of $T_{II\to III}$ for samples B and C is 138°C, which is similar to that of neat isotactic PP,[27] but the value of $T_{II\to III}$ for sample D is lower than 132°C, and all the T_c's studied for sample D are located in crystallization regime II. Sample A has an interme-

TABLE II
***G* Values for the Polyolefin In-Reactor Alloys at Various T_c's**

	G (μm/s)			
T_c (°C)	A	B	C	D
128	0.715	—	2.395	0.335
130	0.330	—	1.340	0.280
132	0.150	3.750	0.785	0.215
134	0.075	1.895	0.440	0.170
136	0.050	0.975	0.250	0.135
138	0.035	0.495	0.210	0.105
140	0.025	0.305	0.160	0.085
142	—	0.255	0.120	0.065
144	—	0.175	0.085	—
146	—	0.100	—	—

TABLE III
σ_e and % Values for the PE/PP and PE/PP/EPR Alloys

Samples	$T_{II\to III}$ (°C)	σ_e (ergcm^2)	q (kJ/mol)
A	134	77	31.9
B	138	62	25.6
C	138	45	18.6
D	≤132	65	26.9

diate $T_{II \rightarrow III}$ value of 134°C. Also, for the PE/PP alloys, sample B has a smaller value of σ_e than sample A, and for the PE/PP/EPR alloys, sample C has a smaller value of σ_e than sample D. As we have known, sample A contains little propylene homopolymer, whereas the weight percentages of the propylene homopolymer, ethylene homopolymer, and ethylene–propylene block copolymer are similar. Moreover, for the PE/PP/EPR alloys, the composition of the block copolymer fraction in sample D is highly asymmetric, although sample D contains more block copolymer fraction. This shows that the distribution of the fractions and the composition of the block copolymer fraction have effects on σ_e. Comparing the values of σ_e for the PE/PP and PE/PP/EPR alloys, we can see that the PE/PP/EPR alloys tend to have smaller σ_e values than the PE/PP alloy, and this indicates that the ethylene–propylene random copolymer may also reduce σ_e of PP. The decrease in the value of σ_e shows that in the melt of the polyolefin in-reactor alloys, PP is at least partially compatible with other components; thus, the folding entropy of PP during crystallization is enhanced. In other compatible blend systems, σ_e of the crystalline component has also been found to decrease as the percentage of the compatible amorphous component increases.[31,32] As a result, a suitable weight percentage and composition of the block copolymer fraction can improve the compatibility of a polyolefin in-reactor alloy, and this is in accordance with the morphology observed after nonisothermal crystallization. Because q is proportional to σ_e, the composition of the alloys affects q and σ_e in a similar way.

CONCLUSIONS

The POM graphs show that the overall morphology of the polyolefin in-reactor alloys varies with the composition and crystallization conditions. The PP alloys containing a suitable block copolymer fraction and a larger amount of PP have a more homogeneous morphology, and the crystalline particles are smaller; this indicates improved compatibility. Quenching also leads to smaller crystallites and a more homogeneous morphology. Isothermal crystallization above the melting temperature of PE reveals that the alloys with higher propylene contents usually have faster spherulitic growth rates. The block copolymer fraction and random copolymer fraction can reduce σ_e of PP in the alloys. The composition of the alloys may also affect the crystallization regime of PP.

References

1. Galli, P.; Haylock, J. C. Prog Polym Sci 1991, 16, 443.
2. Simonazzi, T.; Cecchin, G.; Mazzullo, S. Prog Polym Sci 1991, 16, 303.
3. Galli, P. Prog Polym Sci 1994, 19, 959.
4. Wang, L. X.; Huang, B. T. J Polym Sci Part B: Polym Phys 1991, 29, 1447.
5. Soares, J. B. P.; Hamielec, A. E. Polymer 1995, 36, 1639.
6. Xu, J. T.; Feng, L. X.; Yang, S. L.; Wu, Y. N.; Yang, Y. Q.; Kong, X. M. Polymer 1997, 38, 4381.
7. Mirabella, F. M. J. J Appl Polym Sci Appl Polym Symp 1992, 51, 117.
8. Mirabella, F. M. J. Polymer 1993, 34, 1729.
9. Usami, T.; Gotoh, Y.; Umemoto, H.; Takayama, S. J Appl Polym Sci Appl Polym Symp 1993, 52, 45.
10. Zhang, X. Q.; Olley, R. H.; Huang, B. T.; Bassett, D. C. Polym Int 1997, 43, 45.
11. Cai, H. J.; Luo, X. L.; Chen, X. X.; Ma, D. Z.; Wang, J. M.; Tan, H. S. J Appl Polym Sci 1999, 71, 103.
12. Fan, Z. Q.; Zhang, Y. Q.; Xu, J. T.; Wang, H. T.; Feng, L. X. Polymer 2001, 42, 5559.
13. Feng, Y.; Jin, X.; Hay, J. N. J Appl Polym Sci 1998, 68, 381.
14. Feng, Y.; Hay, J. N. Polymer 1998, 39, 6589.
15. Pires, M.; Mauler, R. S.; Liberman, S. A. J Appl Polym Sci 2004, 92, 2155.
16. Xu, J. T.; Fu, Z. S.; Fan, Z. Q.; Feng, L. X. Eur Polym J 2002, 38, 1739.
17. Xu, J. T.; Ding, P. J.; Fu, Z. S.; Fan, Z. Q. Polym Int 2004, 53, 1314.
18. Amash, A.; Zugenmaier, P. J Polym Sci Part B: Polym Phys 1997, 35, 1439.
19. Yokoyama, Y.; Ricco, T. J Appl Polym Sci 1997, 66, 1007.
20. Allport, D. C.; Jones, W. H. Block Copolymers; Applied Science: London, 1973.
21. Nitta, K.; Kawada, T.; Yamahiro, M.; Mori, H.; Terano, M. Polymer 2000, 41, 6765.
22. Fu, Z. S.; Fan, Z. Q.; Zhang, Y. Z.; Xu, J. T. Polym Int 2004, 53, 1169.
23. Fu, Z. S.; Xu, J. T.; Fan, Z. Q. J Appl Polym Sci 2005, 97, 640.
24. Sacchi, M. C.; Fan, Z. Q.; Forlini, F.; Tritto, I.; Locatelli, P. Macromol Chem Phys 1994, 195, 2805.
25. Lauritzen, J. I.; Hoffman, J. D. J Appl Phys 1973, 44, 4340.
26. Hoffman, J. D.; Davis, G. T.; Lauritzen, J. I. In Treatise on Solid State Chemistry; Hannay, N. B., Ed.; Plenum: New York, 1976; Vol. 3.
27. Clark, E. J.; Hoffman, J. D. Macromolecules 1984, 17, 878.
28. Cheng, S. Z. D.; Janimak, J. J.; Zhang, A.; Cheng, H. N. Macromolecules 1990, 23, 298.
29. Hoffman, J. D.; Miller, R. L.; Marand, H.; Roitman, D. B. Macromolecules 1992, 25, 2221.
30. Hoffman, J. D.; Miller, R. L. Polymer 1997, 38, 3151.
31. Martuscelli, E.; Silvestre, C.; Abate, G. Polymer 1982, 23, 229.
32. El Shafee, E. Polym Int 2004, 53, 249.